Experimental laboratories, test case 2

Analysis of the velocity field in the wake of a circular cylinder

Francesco Derme, Pietro Di Giustino, Pietro Fumagalli

1 Introduction

We analyze the velocity field around a cylinder in a water channel flow, focusing on the wake region. Reference is made to experimental data obtained through the **particle streak velocimetry** (PSV) technique, which essentially relies on seeding the flow with small particles and shooting a video of an illuminated plane of the confined region of the experiment. The camera has a high exposure time, intended as the time duration of a frame, so that each particle leaves a streak on the image. The images are then processed to obtain the velocity field. In this case, the Reynolds number of the cylinder $Re_D = D \cdot \frac{U_\infty}{\nu}$ is within the range of the *sub-critical regime.* Strictly speaking this classification of flow regimes refers to unconfined flows with uniform free-stream inlet which isn't the case here since the cylinder is located in a water channel with finite-size cross section. Still, it's reasonable to expect a behavior similar to that of the unconfined case, therefore it won't be surprising to notice that the flow separates at a certain distance from the front stagnation point causing a recirculation zone to form behind the cylinder and that a turbulent oscillating wake is created by the shedding of two counter-rotating vortexes.

As for the experimental setup: the PSV acquisition system records water flowing from right to left and we will be consistent with this reference in the produced graphs. The framing of the camera, which is the measurement field, is a vertical plane in the mid-section of the channel. The coordinate system of the PSV acquisition has its origin in the top-left corner of the acquisition frame, with the X-axis going from left to right and the Y-axis going from top to bottom.

Symbol	Parameter	Value	Unit
B	Width of the channel	0.5	m
D	Diameter of the cylinder	0.06	m
fs	Sampling frequency	50	Hz
h	Water level in the channel upstream of the cylinder	0.42	m
hb	Distance of the cylinder wall from the channel bottom	0.18	m
Q	Volumetric flow rate of water	35	l/s
res	Resolution of the images	3040	px/m
ρ	Density of water	998	kg/m^3
μ	Dynamic viscosity of water	0.001	Pa $\cdot$ s

During the post-processing of the PSV data, the frame was divided into a regular grid of 30 x 23 uniform cells along the directions X and Y as previously described. The number of time steps is 1499 and the duration of each of them is equal to $\frac{1}{fs}$. The results of the post-processing is made available through the following variables:

Variable	Dimension	Value	Unit
Grid_Xpx	23 x 30	X-coordinates of grid centers in the frame	px
Grid_Ypx	23 x 30	Y-coordinates of grid centers in the frame	px
SXpx	23 x 30 x 1499	X displacement for every time step	px
SYpx	23 x 30 x 1499	Y displacement for every time step	px

A static snapshot of the PSV frame with a ruler close to the cylinder has been taken before running the experiment. The snapshot has been used to estimate the resolution of the image and it will also be useful in turning the pixel-based matrices into the corresponding dimensionless matrices in the new coordinate system centered in the rear stagnation point and directed from left to right, bottom to top.

2 Preliminary analysis

1. We calculate the channel bulk velocity U_b based on quantities measured upstream of the cylinder, $U_b = \frac{Q}{B \cdot h} = 0.1667 \frac{m}{s}$. This velocity is assumed to be the free stream velocity approaching the cylinder, U_∞ so that the Reynolds number $Re_D = \frac{D \cdot U_\infty}{\nu}$ can be calculated. Note that $U_b \neq U_\infty$ since the experiment involves water flowing in a finite-size channel, nonetheless this is a reasonable approximation. The result indicates what, in an unconfined setting, would be the sub-critical regime.

$$5000 < Re_D = \frac{D \cdot U_\infty}{\nu} = 9980 < 3 \cdot 10^5 \tag{1}$$

2. The pixel-based matrices must be turned into proper dimensionless matrices. Reference is made to the coordinate system centered in the rear stagnation point of the cylinder which is "more physically intuitive" than that of the PSV frame. To this aim, we first find the coordinates of the origin of the new coordinate system in the old one in pixels by making use of the reference image, they turn out to be $x = 464$px, $y = 273$px, then turn them in meters diving by the resolution. Now we build two new matrices which contain the centers of the cells expressed in meters according to the new coordinate system, then turn them into dimensionless matrices by normalizing by the diameter of the cylinder. In one step this looks as follows:

$$Grid\_x0\_D = \frac{\text{stagnation\_pt\_coord\_mt}(1) - \frac{Grid\_Xpx}{res}}{D} \tag{2}$$

$$Grid\_y0\_D = \frac{\text{stagnation\_pt\_coord\_mt}(2) - \frac{Grid\_Ypx}{res}}{D} \tag{3}$$

Two matrices containing the displacements in meters according to the new coordinate system also need to be built. To do this we first gather the matrices of the "instantaneous" velocity field by considering that the displacements were measured during the exposition time $\frac{1}{fs}$. Finally we turn them dimensionless by normalizing by the bulk velocity U_b. In one step this looks as follows:

$$u0\_Ub = -1 \cdot \frac{SXpx}{res} \cdot \frac{fs}{U_b} \tag{4}$$

$$v0\_Ub = -1 \cdot \frac{SYpx}{res} \cdot \frac{fs}{U_b} \tag{5}$$

Note that it's improper to talk about *instantaneous velocity field*, indeed the data we have reports the velocity of the seeding particles (albeit with small Stokes number) averaged within the time step $\frac{1}{fs}$.

3 Analysis of the Reynolds-averaged flow field

1. We calculate the Reynolds-averaged velocity field through a time average of the "instantaneous" velocity matrices. Close attention is payed to the many NaN quantities present in the matrices, these are excluded from the average. Their presence is to be expected and due to interpolation problems in the PSV post-processing algorithm as well as to the fact that, during flow, particles might move in and out of plane and suddenly appear or disappear from the frame.

   Of course it's not guaranteed that the number of available frames is enough for the averaged variables to be representative of the Reynolds averaged flow. To test this hypothesis with a quantitative yet arbitrary metric, we define the *stable region* as the region where the cumulative average of a signal is **definitively** within a bound of $\pm 10\%$ of the final average. Then, for a signal to be *converged*, we require the length in seconds of this stable region to be bigger than or equal to 1 second. We use this test on x- and y-velocities in 8 different randomly-sampled points of the domain, cylinder excluded.

Every signal passes the test except for signal 7 whose stable region only lasts 0.14 seconds and signal 8 whose stable region only lasts 0.76 seconds. It's worth noting that an oscillatory behavior is to be expected, especially in the y-velocities, due to the nature of the setup, so for 6 tests to be converged out of 8 is still a good result and we deem our method for numerically approximating Reynolds averages to be acceptable.

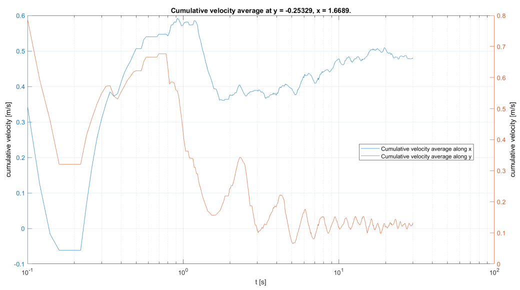

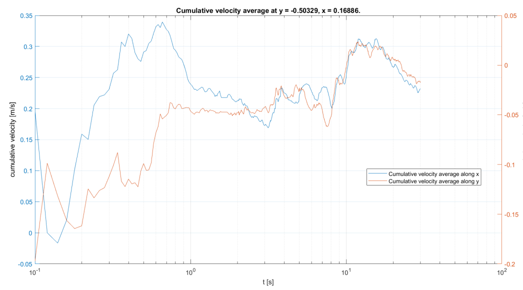

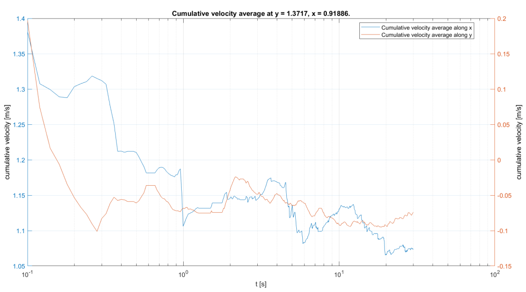

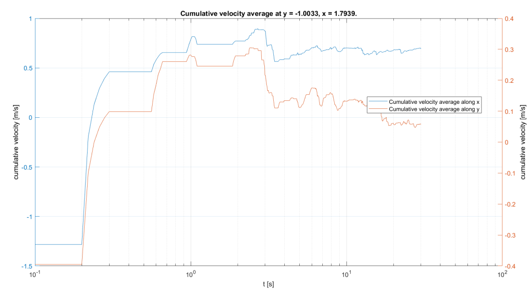

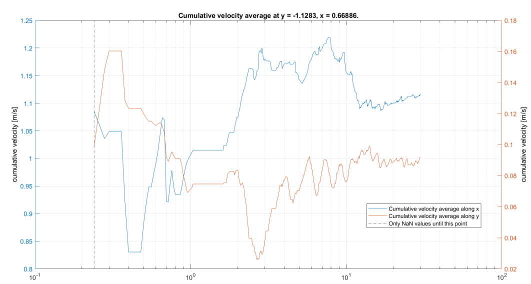

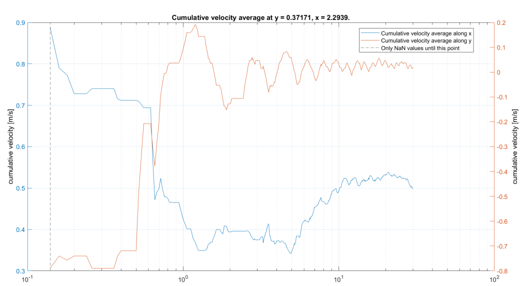

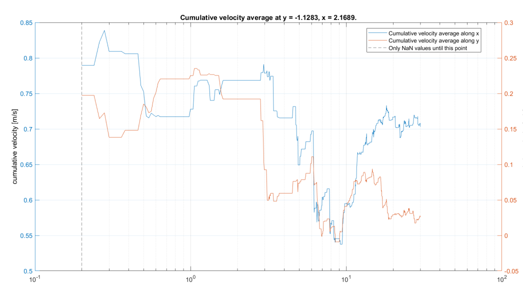

We propose some visualizations of the Reynolds-averaged velocity field by showing the color plot of the Reynolds-averaged velocity magnitude, then we calculate the Reynolds-averaged vorticity field and show the color plot of this variable as well. We also plot the vector map of the Reynolds-averaged velocity field, its streamlines, the $\frac{U_0}{U_b}$ profiles along the horizontal line $\frac{y_0}{D} = 0$ and along the two vertical lines $\frac{x_0}{D} = 0.5$ and $\frac{x_0}{D} = 1.5$, this requires interpolating the grid values at selected space positions. Note that spurious vectors will be found inside of the space occupied by the cylinder. Clearly, these vectors are nonphysical and they are the consequence of perspective errors or issues in the PSV algorithm. They should be ignored.

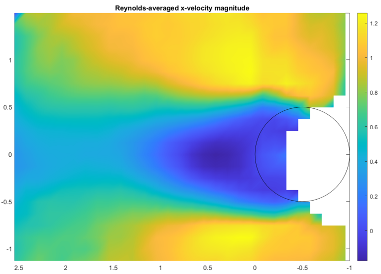
Reynolds-averaged x-velocity magnitude

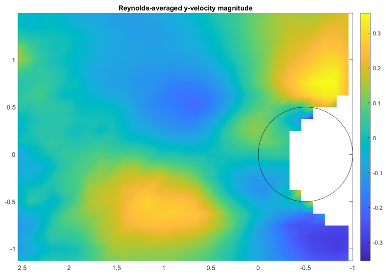
Reynolds-averaged y-velocity magnitude

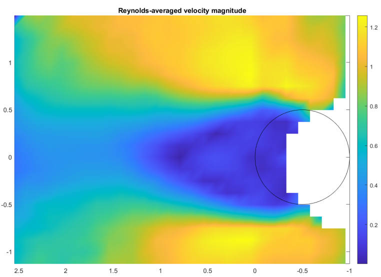
Reynolds-averaged velocity magnitude

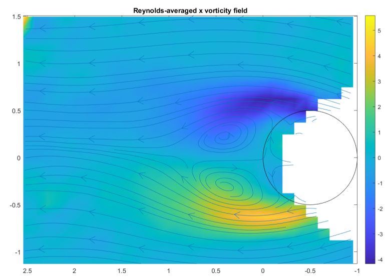
Reynolds-averaged x vorticity field

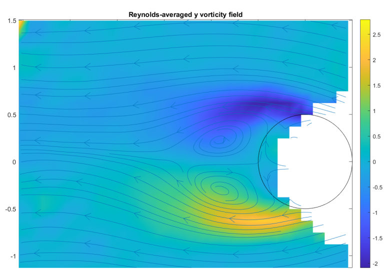
Reynolds-averaged y vorticity field

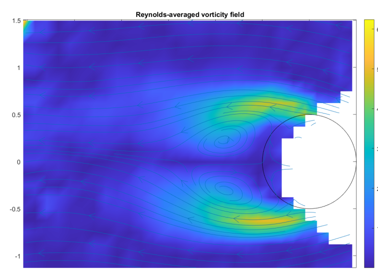
Reynolds-averaged vorticity field

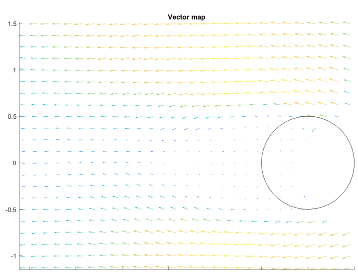
Vector map

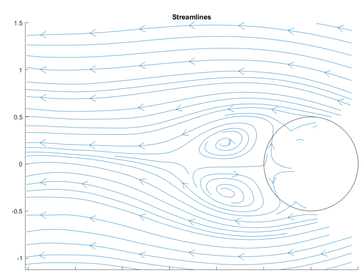
Streamlines

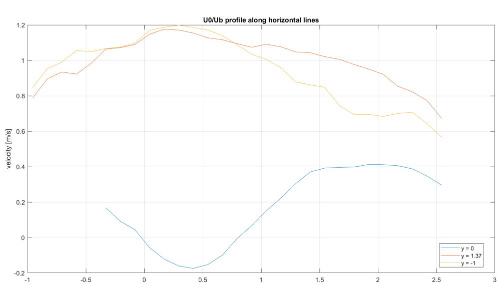
U0/Ub profile along horizontal lines
velocity [m/s]
z [m]
y = 0
y = 1.37
y = -1

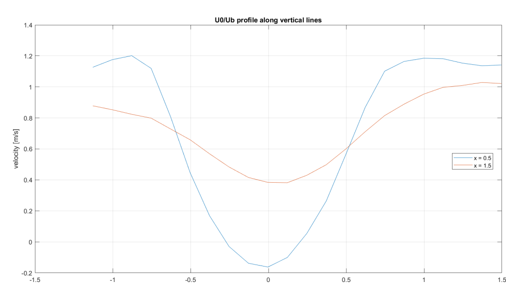
U0/Ub profile along vertical lines
velocity [m/s]
y [m]
x = 0.5
x = 1.5

The x-velocity component is, as we expected, more relevant than the y-component in computing the velocity magnitude. It is at its strongest in the bottom and top regions where water can flow undisturbed by the cylinder, it reaches its minimum behind the obstacle and slowly approaches a uniform distribution towards the end of the frame. The y-component increases near the top of the cylinder and downstream of it in the bottom half of the frame, this testifies to the creation of vortexes and general disturbances in the flow. The asymmetry can be explained with reference to the fact that the cylinder is placed lower than the middle point between tank floor and air, furthermore the fact the the flow is confined from below and unconfined from above is itself cause of the asymmetry. The vorticity field, vector map and streamlines show clearly the path water takes as it evades the cylinder, particularly the last one is a beautiful visualization of the swirling effect that takes place behind the obstacle.

Looking at the U_0 velocity profile along horizontal lines clearly shows that flow at the cylinder is halted, but since mass conservation must hold horizontal velocity increases in other regions, then the profile slowly goes back to being uniform. Looking at the U_0 velocity profile along vertical lines tells the same story from a different perspective: close to the cylinder the velocities massively differ with respect to y, then these differences get smoothed out.

4 Analysis of the dynamic evolution of the flow

1. Even after filtering out the noise due to turbulence there's still an evolution of the flow in time caused by vortex shedding, these are the phenomena we aim to capture in this section. An obvious starting point is the time history of the normalized vertical velocity $\frac{v_0}{U_b}$ in a point around the rear of the cylinder, in particular we choose the point at coordinates $x = 1.418859649122807$, $y = -0.003289473684210$.

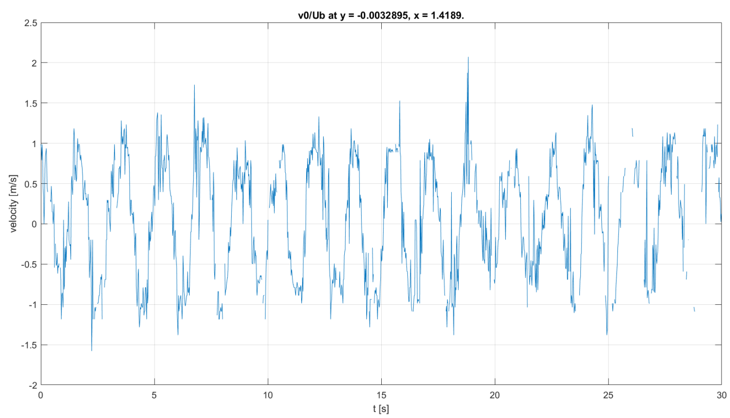

Of course the y-velocity here fluctuates as vortexes swirling in opposite directions periodically detach from the cylinder and drift away.

2. We compute the *Fast Fourier Transfom* (FFT) of the $\frac{v_0}{U_b}$ velocity signal and plot the frequency spectrum. The vortex shedding frequency, f, is approximated as the main peak of the spectrum.

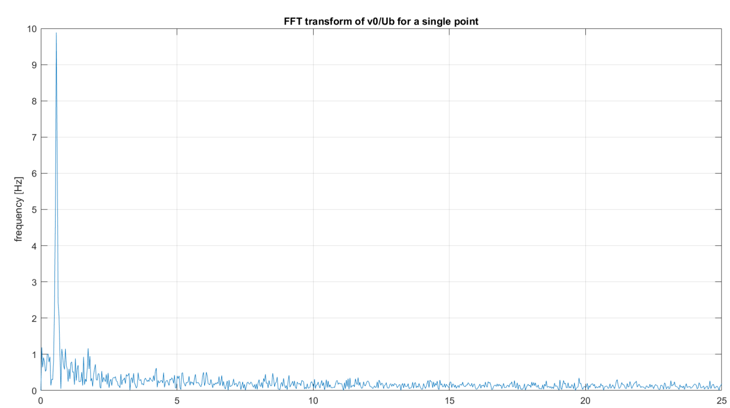

3. An estimate of the characteristic Strouhal number of the oscillating wake can be computed as $Sr = f \cdot \frac{D}{U_b} = 0.20427$ and compared with a reference value from the literature at the same Reynolds number for the unbounded case. This reference solution comes from the paper by Fei et al. (1998) and yields $Sr_F = 0.225$. The quality of fit - good but not perfect - testifies to the similarities and the differences between the two experimental setups: on the one hand Reynolds numbers are identical, but on the other we are testing a confined flow whereas the cited paper studies the flow of air in a wind tunnel where the effect of the walls is negligible.

4. To investigate the sensitivity of the estimated Strouhal number with respect to the initial choice of the monitoring point we overlap the frequency spectra for all the points in the domain. Of course the points located inside the cylinder or those were nothing but NaN values were recorded are excluded from this analysis. This way of proceeding leads the plot to be overcrowded, so we also make a version were only points in the rear section of the cylinder are considered but this, unfortunately, doesn't solve the issue as frequency spectra are sill very varied.

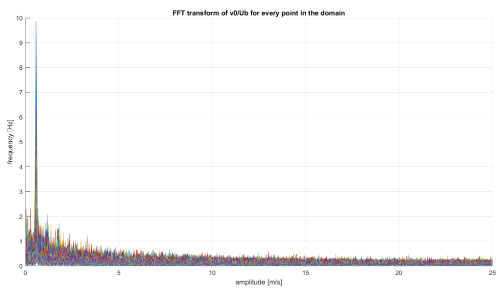

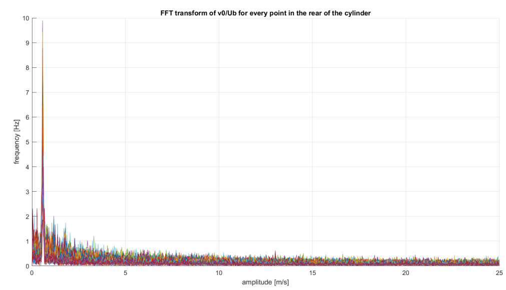

Another proposed approach involves calculating the percentage shift in Strouhal number among different points, this was computed as $(Sr_{max} - Sr_{min}) \cdot \frac{100}{Sr_{max}}$ for both the whole domain and only the rear part of the cylinder. This idea failed as both times the result was 100% indicating that in both cases there existed a point for which the most significant component of the velocity had null frequency. Hence we resort to analyzing the color plot distribution of the vortex shedding frequency.

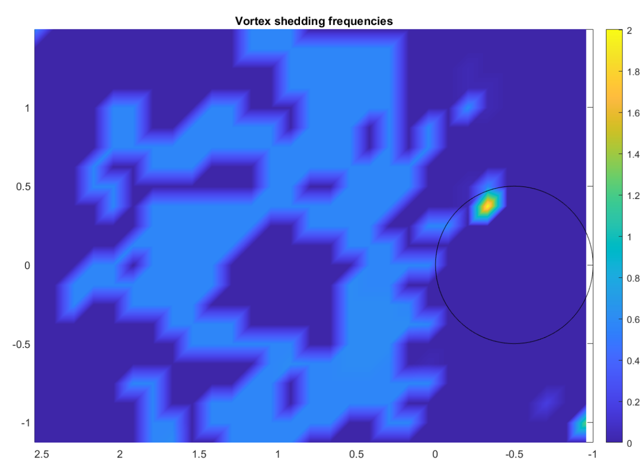

Frequency of vortex shedding seems to be highest at the top of the cylinder. This was foreseeable considering what the Reynolds-averaged y-velocity magnitude plot had shown.

5. After having applied a temporal moving average to the instantaneous velocity field, we analyze the time evolution of the velocity magnitude field, the velocity vector field, the streamlines, and the vorticity field at different time instants by producing corresponding videos. To do so we consider an averaging window of $0.2T$ where $T = \frac{1}{f}$ the vortex shedding period. This choice was made because, in order to capture the vortexes, the time window must be shorter than T, but too short would defeat the purpose of averaging out the effect of turbulence. To convert the averaging window size from seconds to number of frames it's enough to multiply by fs, this yields 18 frames. The videos beautifully show vortex detachment and all the previously-talked-about phenomena.